Chirped pulse Raman amplification in plasma

2011 New J. Phys. 13 063042

(http://iopscience.iop.org/1367-2630/13/6/063042)

New Journal of Physics
The open-access journal for physics

Chirped pulse Raman amplification in plasma

G Vieux, A Lyachev[1], X Yang, B Ersfeld, J P Farmer, E Brunetti, R C Issac, G Raj, G H Welsh, S M Wiggins and D A Jaroszynski[2]
Department of Physics, Scottish Universities Physics Alliance, University of Strathclyde, Glasgow G4 0NG, UK
E-mail: d.a.jaroszynski@strath.ac.uk

New Journal of Physics **13** (2011) 063042 (9pp)
Received 27 January 2011
Published 23 June 2011
Online at http://www.njp.org/
doi:10.1088/1367-2630/13/6/063042

Abstract. Raman amplification in plasma has been proposed to be a promising method of amplifying short radiation pulses. Here, we investigate chirped pulse Raman amplification (CPRA) where the pump pulse is chirped and leads to spatiotemporal distributed gain, which exhibits superradiant scaling in the linear regime, usually associated with the nonlinear pump depletion and Compton amplification regimes. CPRA has the potential to serve as a high-efficiency high-fidelity amplifier/compressor stage.

Contents

1. Introduction

High-power ultra-short pulse lasers have become valuable tools for scientists exploring a wide range of phenomena and developing new technologies such as ultra-compact wakefield accelerators [1] and compact light sources [2]. Modern high-power lasers rely on chirped pulse amplification (CPA), a technique originally applied to lasers in the 1980s [3] to avoid damage

[1] Current address: Central Laser Facility, Rutherford Appleton Laboratory, Chilton OX11 0QX, UK.
[2] Author to whom any correspondence should be addressed.

to optical components. Optical parametric chirped pulse amplification (OPCPA) [4] has been proposed as a way of increasing both the bandwidth and the power of high-power amplifiers. However, the maximum output power of both CPA and OPCPA amplifiers is limited to several petawatts by the maximum intensities sustainable by optical components.

This limitation has led to the suggestion of the use of stimulated Raman backscattering in plasma as an alternative amplifying medium [5] because plasma can sustain very high fields. Stimulated Raman scattering (SRS) occurs when an incident electromagnetic wave, with a frequency ω_0 and wave vector $\mathbf{k_0}$, resonantly decays into a backscattered electromagnetic wave (ω_1, $\mathbf{k_1}$) and a plasma wave ($\omega_\mathrm{p} = \sqrt{ne^2/\epsilon_0 m}$, $\mathbf{k_p}$), with c being the speed of light and e and m the electron charge and mass, respectively. It only occurs over a narrow frequency range when the resonance conditions $\omega_0 \approx \omega_1 + \omega_\mathrm{p}$ and $\mathbf{k_0} \approx \mathbf{k_1} + \mathbf{k_p}$ are satisfied [6]. In the linear SRS regime, i.e. at moderate intensities ($\leqslant 10^{14}\,\mathrm{W\,cm^{-2}}$ for $\lambda = 800\,\mathrm{nm}$), the amplitude of the seed grows exponentially as $a_1 \mathrm{e}^{\gamma_0 t}$, where $\gamma_0 = a_0(\omega_0\omega_\mathrm{p}/2)^{1/2}$ is the growth rate for circularly polarized monochromatic beams, t is the duration of the interaction [7, 8] and $a_{0,1}$ are the normalized vector potentials given by $a_{0,1} = eA_{0,1}/mc$, with $A_{0,1}$ being the vector potential amplitudes. Despite this significant gain, Raman amplification can be diminished by several concurrent phenomena such as spontaneous Raman backscattering, leading to early pump depletion, Raman forward scattering, temperature increase due to inverse bremsstrahlung (IB) heating, wave breaking, Landau damping, particle trapping, etc [9]. Also, in the linear regime, the intrinsically narrow bandwidth of the Raman instability, equal to $2\gamma_0$ [8], and its convective instability [10], lead to temporal stretching of the seed [6], reducing its usefulness as a short-pulse amplifier. To avoid these limitations, Shvets and co-workers [6, 11, 12] have proposed taking advantage of the nonlinearity of the medium at high intensities to produce soliton-like ultra-short pulses through pump depletion or, at higher intensities, by operating in the Compton or superradiant [13] regime where the ponderomotive force exceeds that of the plasma wave, i.e. when the bounce frequency, $\omega_\mathrm{B} = 2\omega_0\sqrt{a_0 a_1}$, of plasma electrons in the ponderomotive well exceeds ω_p [11, 12]. In this regime, the seed intensity grows in proportion to the square of the plasma density and the duration decreases as $|a_1|^{1/2}$.

Raman amplification in plasma has been experimentally studied in capillaries [14, 15] and gas jets [16–19] and also in the Compton regime [20]. More recently, an energy gain of 350 has been observed in a 2 mm-long double-pass SRS amplifier [18, 19], where the seed energy increased from 16 μJ to 5.6 mJ, while the pulse compressed from 500 to 50 fs. While promising, the energy transfer efficiency of this amplifier was only 6.4% when calculations and simulations predict high efficiency in the pump depletion regime. Moreover, these published results are still far away from demonstrating the required efficiency for a useful amplifier. To further develop SRS as a new type of amplifier, it is important to explore the factors limiting the overall gain. One common feature of all these experiments is that the pump beam is temporally stretched by frequency chirping. This results in detuning, whose effect has been identified as limiting the amplification efficiency [21].

In this paper, we present the first experimental investigation on the role of frequency chirp in the linear regime of Raman amplification in a preformed uniform plasma channel.

2. The principle of chirped pulse Raman amplification (CPRA)

An important observation of our work is that the pump chirp leads to a spatiotemporal frequency distribution of the gain, which restricts the effective interaction length independent of the overall

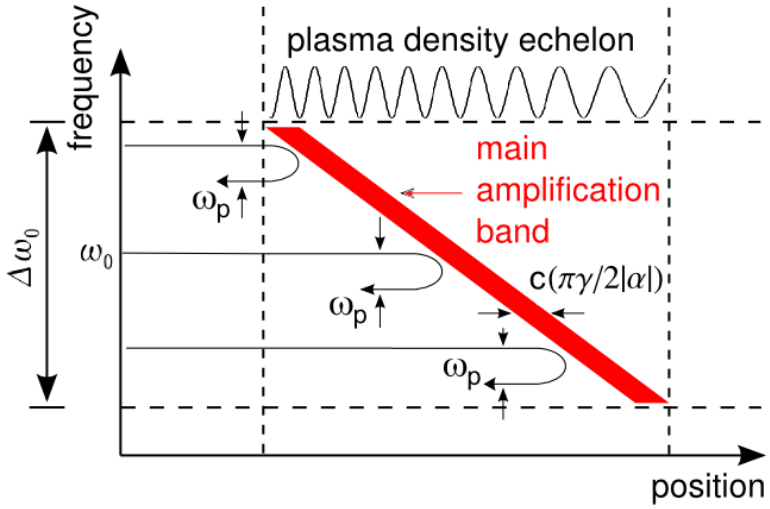

Figure 1. Schematic diagram of a chirped plasma grating formed by the beating of the pump and seed beams at a given instant. The pump beam propagates from left to right in the figure. The amplification band (in red) shows the position in the plasma where each pump frequency is backscattered while down-shifted by the plasma frequency. The width of the band illustrates the distance over which backscattering occurs. ω_p is the plasma frequency and $\Delta\omega_0$ is the pump spectral bandwidth representing the available bandwidth for amplification.

plasma length, resulting in a gain factor that is proportional to the pump intensity rather than the amplitude, as would be the case for a monochromatic pump. This leads to the seed growth exhibiting superradiant scaling, which is an unusual observation for the linear regime. If we consider both pump and seed to be monochromatic, the gain coefficient, γ, depends on the detuning $\delta = \omega_0 - \omega_1 - \omega_p$: $\gamma(\delta) = \sqrt{\gamma_0^2 - \delta^2}$. In the case when the pump pulse frequency chirp rate is α, such that $\omega_0 = \omega_0^{(0)} + \alpha(t + z/c)$, the chirp determines the longitudinal position at which each frequency component of the seed will be amplified. This is because the local detuning, $\delta(z, t) \simeq \alpha(t + z/c)$, only allows the plasma wave to grow while $|\delta(z, t)| \leqslant \gamma_0$, i.e. while the spectral component remains within the resonance bandwidth. This has the effect of distributing the gain in both frequency and position, as shown schematically in figure 1, resulting in broad band-width amplification with a gain that is independent of the plasma channel length. The amplification of each spectral component is restricted to a distance (or region) $\delta z \simeq c(\pi|\gamma_0/2\alpha|)$ by detuning imposed by the chirp [22]. The fields scattered off the plasma wave superpose coherently just behind the seed, but dephase with increasing distance from it. Thus both the seed amplitude and the spectral bandwidth grow in proportion to z, which contrasts with the continual stretching of the seed profile expected for a monochromatic pump. The scattered fields effectively carry out a Fourier transform of the seed 'on the fly', which leads to self-similar growth that exhibits superradiant scaling usually associated with the nonlinear Raman and Compton regimes [22]. The evolution of the seed bandwidth is limited by the overlap of the bandwidths of the seed and the pump. The overall gain bandwidth depends on the pump intensity rather than its amplitude since the saturation of the growth of the plasma wave has the same dependence. Such a dependence will also occur with a monochromatic pump and a plasma with a density gradient [12].

3. Experimental results and discussion

To observe chirped pulse Raman amplification (CPRA), an experiment with two collinear counterpropagating beams in a plasma channel was set up using the terahertz to optical pulse source (TOPS) high-power laser system [23], which provides a 350 mJ, 170 ps chirped pump beam at $\lambda_0 = 800$ nm with a spectral bandwidth $\Delta\lambda \approx 25$ nm, at a chirp rate $\alpha = \Delta\omega/\Delta T \approx 4.47 \times 10^{23}\,\mathrm{s}^{-2}$. Part of the beam, providing the seed, is compressed to 600 fs in an adjustable grating compressor before passing through a BK7 glass plate to increase the bandwidth by $\sim$10% by self-phase modulation. Both seed and pump beams are focused on either ends of a 4 cm long, 300 μm internal diameter plasma channel waveguide. A variable delay line on the pump beam enables temporal overlap of the two beams inside the plasma, i.e. the delay line acts as a frequency selector. The plasma channel, mounted on a five-axis stage, is formed by a high-voltage discharge in a H_2-filled capillary [24, 25]. The plasma cools against the capillary wall to form a parabolic radial density distribution with an on-axis minima. The density is given by $N(r) = N(0) + \Delta N(r/r_m)^2$. Here $N(0)$ is the on-axis density, ranging from 5×10^{17} to $2 \times 10^{18}\,\mathrm{cm}^{-3}$, and ΔN the density increase at the capillary wall, i.e. when $r = r_m$, where r_m is the capillary radius. This gives a ratio $\omega_\mathrm{p}/\omega_0 \approx 2\%$. The laser beam couples to the fundamental mode of the waveguide provided the beam waist, radius at $1/\mathrm{e}^2$ in intensity, $w_M = (r_m^2/(\pi r_\mathrm{e}\Delta N))^{1/4}$, where r_e is the classical electron radius. The plasma channel enables an increase of the effective interaction length beyond the Rayleigh length. Following interaction, a small fraction of the seed is split off to (i) a spectrometer to measure the gain as a function of wavelength, (ii) a single-shot auto-correlator to observe the change in the seed duration and (iii) an imaging system to measure the laser spot shape. At the entrance of the channel the maximum pump and seed energies are 220 and 3 mJ, respectively, with a beam waist $\sim$45 μm. The transmission through the channel exceeds 80%. The pump and seed normalized vector potentials are $a_0 = 2.4 \times 10^{-3}$ and $a_1 = 4.9 \times 10^{-3}$, respectively, leading to the product $|a_0 a_1|$ a factor 8.5 below the threshold for entering the superradiant regime, thus ensuring operation in the linear regime. The gain coefficient, $\gamma_0 = 5.58 \times 10^{11}\,\mathrm{rad\,s}^{-1}$, gives a gain length for each seed frequency of $\approx$1 mm that would theoretically result in an intensity growth of 900% for cold plasma and properly frequency-detuned pump and seed.

To establish the mechanism leading to amplification distributed along the plasma channel, the gain has been measured as a function of the relative delay between the seed and pump pulses. For these measurements, the plasma density was $n = 6.5 \times 10^{17}\,\mathrm{cm}^3$ measured by using the frequency difference between the peak gain and the peak loss, equal to $2\omega_\mathrm{p}$ as shown in figure 2 (right). For such a low density, Landau damping and wave breaking reduce the gain. However, obtaining highest gain is not the main objective of the present study. Results are presented in figure 2 (left), where 40 spectra are averaged for each data point because of gain fluctuations due to variations in the pump energy, laser beam pointing and plasma density variations caused by timing jitter of the plasma channel electrical discharge. The spectral gain is given by $g(\lambda) = (I'(\lambda) - I(\lambda))/I(\lambda)$, where I' and I are spectral intensities with and without the pump beam, respectively. As seen in figure 2, seed amplification can be divided into three distinct regions, (A), (B) and (C), as a function of the relative pump–seed delay. The seed pulse experiences loss in the blue part of its spectrum in (A), both gain and loss in region (B) and gain in the red part of its spectrum in (C). This is a direct consequence of using a chirped pump beam since a change in the relative delay enables frequency mapping. The Manley–Rowe relation [26] only allows energy to flow from high- to low-frequency waves. Therefore, when

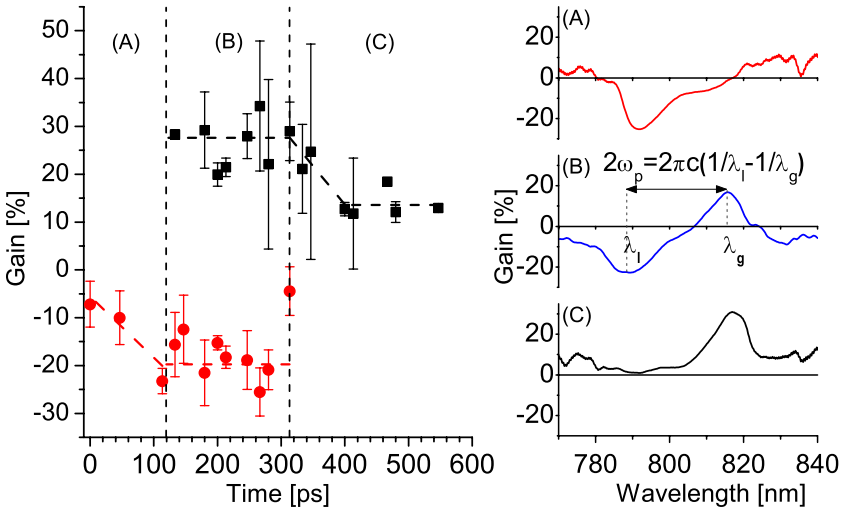

Figure 2. Gain measurements: (left) gain at the Stokes (square) and loss at anti-Stokes (circle) wavelengths as a function of relative delay; (right) spectral gain curve examples for each of the three regions. Spectral gain curves in region (B) are used to calculate the plasma density.

the seed beam collides with the rear of the pump beam (higher frequencies), under proper frequency detuning, the low frequencies of the seed are amplified. Conversely, interaction with the front of the pump beam leads to depletion of the high-frequency part of the seed, reversing the roles of the pump and the seed. Gain and loss of up to 30% are observed. However, a 10% increase in the transmission of the seed through the capillary is observed in region (C). This increase has been ascribed to IB heating by the pump, which causes a reduction in absorption of the seed. Assuming an initial temperature of the plasma of 5 eV due to the creation of the plasma channel [27], a theoretical absorption of $\sim 5\%$ of the seed energy is expected due to IB heating [28]. For the longer delays in region (C) the pump has passed through the capillary before the seed arrived at the entrance. The seed, therefore, propagates in a plasma that has been pre-heated by the pump to a temperature of approximately 50 eV. For such a temperature, the seed absorption can be neglected, which results in the observed increase in transmission, in agreement with our estimates. Also, it has to be noted that the transverse ponderomotive force of the pump beam could decrease the on-axis plasma density, modifying the plasma channel transmission, independent of any Raman gain. From a careful analysis, it is found that the on-axis density is reduced by about 1.7%, while the curvature increases by 15%, corresponding to a reduction in the matched spot size of about 4%. This change has negligible impact in our experiments.

Further evidence of distributed gain and of superradiance has been observed in the dependence of gain on pump intensity. The intensity grows as $\sim e^{\pi\gamma^2/\alpha}$, which depends on the intensity of the pump pulse and not on the amplitude because $\gamma_0^2 \propto a_0^2$. Figure 3 shows the gain measured as a function of a_0^2. The solid line is a fit to γ_0^2/α, while the dotted line represents the scaling, $\gamma_0\tau$, expected for a monochromatic pump beam of duration τ. This measured scaling is evidence that superradiant growth of the seed pulse occurs in a linear chirped pulse Raman amplifier [22].

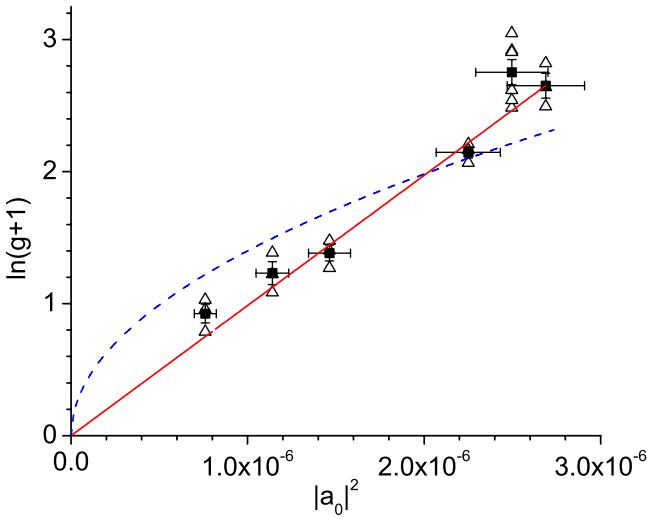

Figure 3. Intensity dependence of the gain. Experimental data points (triangles) are single-shot measurements, while the black squares represent their mean values. The solid (dashed) line is a fit to a linear dependence on pump intensity (amplitude).

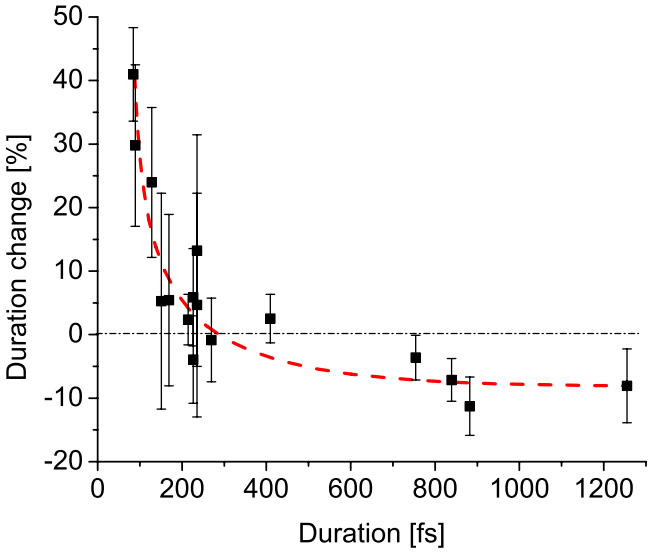

Figure 4. Pulse duration change versus initial pulse duration.

The variation in the amplified seed duration was studied as a function of the initial seed duration, varying from 80 fs to 1.2 ps, with a pump a_0 of 2.7×10^{-3}. For seed pulse durations below 500 fs, the amplified seed appears to be stretched, with a relative duration that increases as the initial pulse duration decreases, as illustrated in figure 4. For example, there is a 40% increase in pulse duration for a 80 fs seed. However, for seed pulses longer than 500 fs, the seed pulse appears to be compressed by a constant compression factor of $\sim$10%. As previously shown, this is because only part of the seed spectrum is amplified. For a short seed pulse this leads to a temporal lengthening. However, conversely, when the seed is long and chirped the frequencies are spatially distributed, leading to an effective compression of the seed pulse.

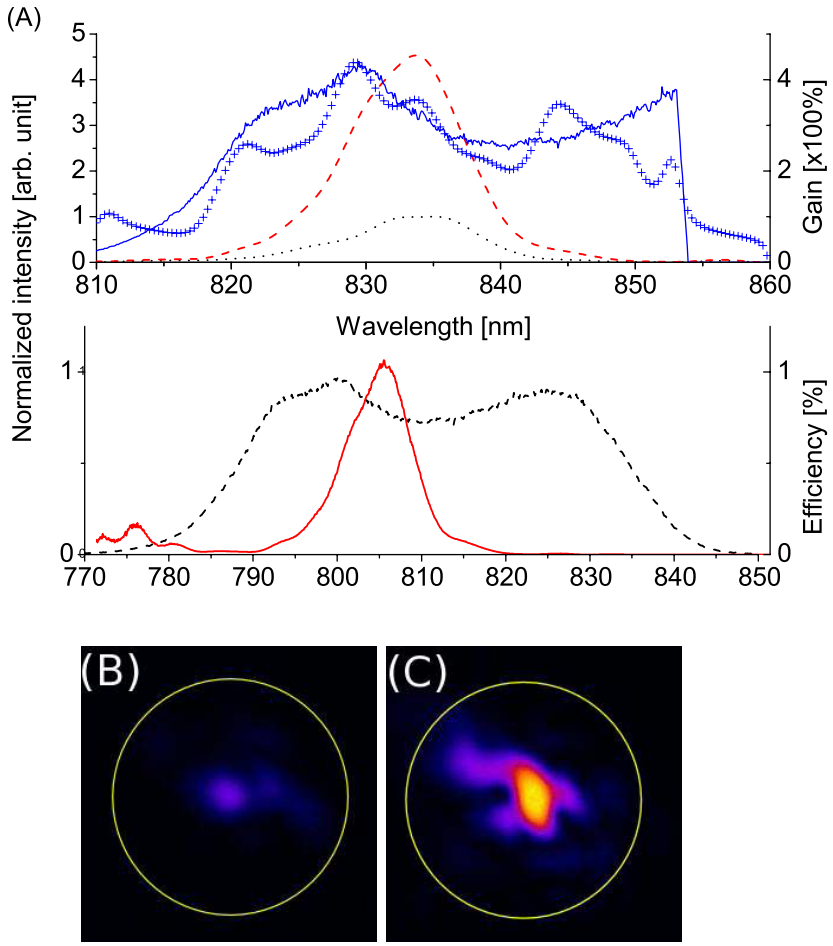

Figure 5. Higher gain measurement. (A) Spectral gain and energy transfer efficiency. Top: the initial (dots) and amplified (dashes) seed spectra with measured (crosses) and calculated (solid line) gain curves. Bottom: the pump spectrum (dashes) with the energy transfer efficiency curve (solid line). (B) Initial seed output. (C) Amplified seed output. In (B) and (C), the circles represent the capillary output.

While the aim of this paper is to clearly demonstrate CPRA, and not to demonstrate highest gain, it is interesting to note that significant amplification can still be achieved for a properly frequency-detuned seed. Using an upgraded laser front-end, peak intensity gains of $\approx 400\%$ have been measured using a 45 nm bandwidth, 300 ps, 350 mJ pump beam and a 200 fs, 250 μJ seed beam, with a plasma density of 2×10^{18} cm^{-3}, as illustrated in figure 5. Amplification is observed with an energy gain of 400% over the full spectral bandwidth while preserving the seed pulse duration. The measured gain is consistent with the expected gain calculated from the pump spectrum. The sharp fall to zero of the gain represents the output edge of the capillary. Also, the efficiency, $\eta(\lambda)$, of the amplifier is determined as a function of wavelength by calculating the energy transferred from the pump to the seed, taking into account the difference in frequency imposed by the resonance condition. In the low gain regime, a typical efficiency of $\sim 1\%$ is measured; however, 5% has also been achieved using a 12 mJ seed beam [29].

4. Conclusion

In conclusion, we have demonstrated that optical chirp of both the pump and the probe plays an important role in the Raman amplification scheme. The gain is spectrally and temporally distributed along the plasma with an interaction duration for each spectral component limited to $\pi|\gamma_0/2\alpha|$ and a gain proportional to the pump intensity. Under those conditions the seed growth exhibits superradiant scaling in the linear regime, which explains why apparent nonlinear growth has been observed previously when energy transfer is low. Furthermore, seed duration measurements should be carefully cross-checked with spectrometer measurements to validate real seed temporal compression. Finally, the measured single-pass efficiencies in an underdense plasma show that linear CPRA has the potential, with suitable scaling of the pump and seed energies, to serve as a high-efficiency high-fidelity amplifier/compressor stage for high-power laser amplifiers within constraints set by wave breaking [30]. CPRA could be a means of controlling the amplification process from the Raman linear regime to the Raman nonlinear regime or Compton regime, which is a necessary step if one starts with a low-energy seed.

Acknowledgment

We acknowledge support from the Engineering and Physical Sciences Research Council, UK.

References

[1] Tajima T and Dawson J 1979 Laser electron accelerator *Phys. Rev. Lett.* **43** 267
[2] Jaroszynski D A and Vieux G 2002 Coherent radiation sources based on laser plasma accelerators *AIP Conf. Proc.* **647** 902
[3] Strickland D and Mourou G 1985 Compression of amplified chirped optical pulses *Opt. Commun.* **56** 219
[4] Ross I N, Matousek P, Towrie M, Langley A J and Collier J L 1997 The prospects for ultrashort pulse duration and ultrahigh intensity using optical parametric chirped pulse amplifiers *Opt. Commun.* **144** 125
[5] Shvets G, Fisch N J, Pukhov A and Meyer-ter Vehn J 1998 Superradiant amplification of an ultrashort laser pulse in a plasma by a counterpropagating pump *Phys. Rev. Lett.* **81** 4879
[6] Malkin V M, Shvets G and Fisch N J 2000 Ultra-powerful compact amplifiers for short laser pulses *Phys. Plasmas* **7** 2232
[7] Forslund D W, Kindel J M and Lindman E L 1975 Theory of stimulated scattering processes in laser-irradiated plasmas *Phys. Fluids* **18** 1002
[8] Kruer W 1988 *The Physics of Laser Plasma Interaction* (Reading, MA: Addison-Wesley)
[9] Berger L R, Clark D S, Sodolov A A, Valeo E J and Fisch N J 2004 Inverse bremsstrahlung stabilization of noise in the generation of ultrashort intense pulses by backward Raman amplification *Phys. Plasmas* **11** 1931
[10] Bobroff D L and Haus H A 1967 Impulse response of active coupled wave systems *J. Appl. Phys.* **38** 390
[11] Shvets G, Wurtele J S and Shadwick B A 1997 Analysis and simulation of Raman backscatter in underdense plasmas *Phys. Plasmas* **4** 1872
[12] Malkin V M, Shvets G and Fisch N J 1999 Fast compression of laser beams to highly overcritical powers *Phys. Rev. Lett.* **82** 4448
[13] Dicke R H 1954 Coherence in spontaneous radiation processes *Phys. Rev.* **93** 99
[14] Ping Y, Geltner I, Morozov A, Fisch N J and Suckewer S 2002 Raman amplification of ultrashort laser pulses in microcapillary plasmas *Phys. Rev.* E **66** 046401
[15] Balakin *et al* 2004 Laser pulse amplification upon Raman backscattering in plasma produced in dielectric capillaries *JETP Lett.* **80** 12

[16] Ping Y, Geltner I and Suckewer S 2003 Raman backscattering and amplification in a gas jet plasma *Phys. Rev.* E **67** 016401
[17] Cheng W *et al* 2005 Reaching the nonlinear regime of Raman amplification of ultrashort laser pulses *Phys. Rev. Lett.* **94** 045003
[18] Ren J, Cheng W, Li S and Suckewer S 2007 A new method for generating ultraintense and ultrashort laser pulses *Nat. Phys.* **3** 732
[19] Ren J, Li S, Morozov A, Suckewer S, Yampolsky N A and Malkin V M 2008 A compact double-pass Raman backscattering amplifier/compressor *Phys. Plasmas* **15** 056702
[20] Dreher M, Takahashi E, Meyer-ter Vehn J and Witte K J 2004 Observation of superradiant amplification of ultrashort laser pulses in a plasma *Phys. Rev. Lett.* **93** 095001
[21] Yampolsky N A, Fisch N J, Malkin V M, Valeo E J, Lindberg R, Wurtele J, Ren J, Li S, Morozov A and Suckewer S 2008 Demonstration of detuning and wavebreaking effects on Raman amplification efficiency in plasma *Phys. Plasmas* **15** 113104
[22] Ersfeld B and Jaroszynski D A 2005 Superradiant linear Raman amplification in plasma using a chirped pump pulse *Phys. Rev. Lett.* **95** 165002
[23] Jaroszynski D A *et al* 2000 The Strathclyde terahertz to optical pulse source (TOPS) *Nucl. Instrum. Methods Phys. Res.* A **445** 317
[24] Spence D J and Hooker S M 2001 Investigation of a hydrogen plasma waveguide *Phys. Rev.* E **63** 015401
[25] Jaroszynski D A *et al* 2006 Radiation sources based on laser–plasma interactions *Phil. Trans. R. Soc.* A **364** 689
[26] Manley M and Rowe H E 1956 Some general properties of nonlinear element—part I. General energy relations *Proc. IRE* **44** 904
[27] Bobrova N, Esaulov A, Sakai J I, Sasorov P, Spence D, Butler A, Hooker S and Bulanov S 2001 Simulations of a hydrogen-filled capillary discharge waveguide *Phys. Rev.* E **65** 016407
[28] Hora H and Wilhelm H 1970 Optical constants of fully ionized hydrogen plasma for laser radiation *Nucl. Fusion* **10** 111
[29] Vieux G, Yang X, Lyachev A, Ersfeld B, Farmer J, Brunetti E, Wiggins M, Issac R, Raj G and Jaroszynski D A 2009 Chirped pulse Raman amplification in plasma: high gain measurements *Proc. SPIE* **7359** 73590R
[30] Trines R M G M, Fiúza F, Bingham R, Fonseca R A, Silva L O, Cairns R A and Norreys P A 2010 *Nat. Phys.* **7** 239